

# Time-Resolved Dynamics of Stable Open- and Closed-Shell Neutral Radical and Oxidized Tripyrrindione Complexes

*Byungmoon Cho<sup>a</sup>, Alicia Swain<sup>a</sup>, Ritika Gautam<sup>a,b</sup>, Elisa Tomat<sup>a</sup> and Vanessa M. Huxter<sup>\*a,c</sup>*

a. Department of Chemistry and Biochemistry, University of Arizona, Tucson, Arizona, 85721

b. Current address: Department of Chemistry, Indian Institute of Technology Kanpur, Kanpur  
208016, India

c. Department of Physics, University of Arizona, Tucson, Arizona, 85721

## **Corresponding Author**

\*Vanessa M. Huxter

[vhuxter@arizona.edu](mailto:vhuxter@arizona.edu)

(520) 621-2115

## ABSTRACT

Stable open- and closed-shell Pd(II) and Cu(II) complexes of hexaethyl tripyrrin-1,14-dione (TD1) produce triplet, doublet or singlet states depending on the metal center and the redox state of the ligand. Pd(II) and Cu(II) form neutral TD1 complexes featuring ligand-based radicals, thus resulting in doublet and triplet states, respectively. The reversible one-electron oxidation of the complexes removes an unpaired electron from the ligand, generating singlet and doublet states. The optical properties and time-resolved dynamics of these systems are studied here using steady-state and ultrafast transient absorption (pump-probe) measurements. Fast relaxation with recovery of the ground state in 10s of picoseconds is observed for the copper neutral radical and oxidized complexes as well as for the palladium neutral radical complex. Significantly longer timescales are observed for the oxidized palladium complex. The ability to tune the overall spin state of the complexes through their stable open shell configurations as well as the reversible redox activity of the tripyrrolic systems makes them particularly interesting for catalytic applications as well as exploring magnetism and conductivity properties.

## INTRODUCTION

In photosynthetic systems, tetrapyrrolic compounds form a primary class of light harvesting pigments,<sup>1</sup> from linear bilins in cryptophyte antennas<sup>2, 3</sup> to the macrocyclic chlorin or bacteriochlorin-based chlorophyll<sup>4</sup> and bacteriochlorophyll.<sup>5</sup> Numerous linear or macrocyclic oligopyrroles, including tetrapyrrolic porphyrins in heme, are found in nature in a variety of roles. Many oligopyrrolic molecules have the capacity to bind metals, often producing redox-active complexes. The ability of these systems to accept or donate electrons plays a central role in biological processes as diverse as water splitting in photosynthesis to enzymatic catalysis and metabolism.

While tetrapyrrolic molecules are common in biological systems, tripyrroles are comparatively rare. Examples of naturally occurring tripyrroles include prodiginines<sup>6, 7</sup> and some heme metabolites such as uroerythrin.<sup>8, 9</sup> Although tripyrroles are rather uncommon in nature, they are effective tridentate ligands for metal coordination<sup>10, 11</sup>.

In the current paper, we present the ultrafast dynamics of the tripyrrolic ligand, hexaethyl tripyrrin-1,14-dione (TD1),<sup>12-14</sup> bound to either a copper(II) or palladium(II) center.<sup>15-17</sup> Tripyrrindiones have the structural scaffold of metabolite uroerythrin and they are related to the family of tripyrrins and other linear tripyrroles.<sup>18, 19</sup> In addition, recent studies have shown that tripyrrindiones are capable of hosting delocalized unpaired electrons and undergo reversible ligand-based redox chemistry in metal complexes that are stable at room temperature.<sup>16, 17</sup> Due to their ability to accommodate unpaired spins on both the metal and the ligand, the tripyrrindione complexes can form stable closed- and open-shell configurations with singlet, doublet, or triplet ground and excited states depending on the nature of the metal center and the overall redox state of the complex.

The TD1 ligand binds in a meridional tridentate fashion through the three pyrrolic nitrogen donors, as shown in Figure 1, forming planar complexes with Pd(II), Ni(II) and Cu(II) ions.<sup>2</sup> A water molecule is bound to the fourth coordination site in the square planar structure. This aqua ligand is hydrogen-bonded to the carbonyl groups of the tripyrrolic ligand and cannot be easily replaced by chemical or electrochemical methods. Spectroscopic and electrochemical data have shown that the tripyrindione ligand in these neutral complexes binds as a dianionic radical featuring an unpaired electronic spin that is delocalized throughout the  $\pi$  system of the ligand.<sup>16, 17</sup> Complexes of tripyrindione in other redox states (i.e., coordinating as a monoanionic or trianionic diamagnetic system) have also been reported.<sup>15, 16</sup> Tripyrindiones, therefore, act as redox-active ligands and can expand the number of available electrons for redox processes beyond the metal center.<sup>11</sup> In addition, complexation with transition metal ions offers possibilities to form complex structures including coordination polymers and  $\pi$ -stacked dimers.<sup>15, 20, 21</sup>

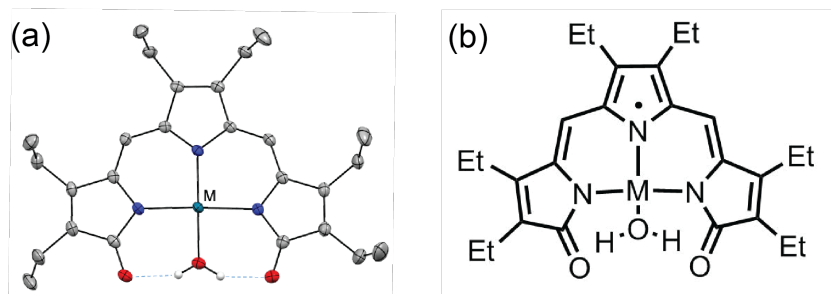


**Figure 1:** Structure of the TD1-metal complexes with coordinated water molecule. In both panels, the M label represents Pd(II) or Cu(II). The crystal structure of [Pd(TD1\*)(H<sub>2</sub>O)] is shown in panel (a). Carbon-bound hydrogen atoms in calculated positions are omitted for clarity (CCDC 1400990). Panel (b) shows the molecular structure of the neutral radical TD1-metal complexes. The unpaired spin density is delocalized over the entire ligand system.

In this paper, we present steady-state and femtosecond time-resolved pump–visible continuum probe measurements of TD1 complexes of copper and palladium in both the neutral radical and oxidized forms. One-electron oxidization of the neutral radical copper and palladium complexes removes an electron from the ligand, leaving the oxidation state of the central metal unchanged. The series of complexes studied here, comprising neutral radical and oxidized forms with Cu(II)  $d^9$  and Pd(II)  $d^8$  metal centers, allow us to compare the effects of changing overall spin quantum number and exchange coupling on the ultrafast electronic dynamics. The tripyrrolic ligands can participate in both one-electron oxidation and reduction independent of the metal center, demonstrating their ability to act as redox-active non-innocent ligands and to host stable ligand-based radicals. Here we abbreviate the neutral radical  $d^9$  tripyrrindione–Cu(II) complex  $[\text{Cu}(\text{TD1}^\bullet)(\text{H}_2\text{O})]$  and the  $d^8$  tripyrrindione–Pd(II) complex  $[\text{Pd}(\text{TD1}^\bullet)(\text{H}_2\text{O})]$  as TD1–Cu and TD1–Pd, respectively. The oxidized, cationic complexes  $[\text{Pd}(\text{TD1})(\text{H}_2\text{O})]^+$  and  $[\text{Cu}(\text{TD1})(\text{H}_2\text{O})]^+$ , both of which have a  $[\text{BF}_4]^-$  counter ion, are abbreviated as TD1–Cu–Ox and TD1–Pd–Ox.

Using steady-state linear absorption and broadband-probe transient absorption measurements, the optical properties and ultrafast dynamics of the electronic relaxation pathways were measured as a function of solvent dependence and oxidation state. We present a series of transient absorption measurements of the neutral radical and oxidized complexes in acetonitrile (MeCN), *N,N*-dimethylformamide (DMF) and toluene. The ultrafast dynamics were mapped using global analysis<sup>22</sup> of the transient absorption measurements.

## EXPERIMENTAL METHODS

The redox-active TD1-Pd and TD1-Cu as well as one-electron oxidized TD1–Cu–Ox and TD1–Pd–Ox complexes were synthesized according to previously reported methods.<sup>16, 17</sup> The metal

complexes were dissolved in dry/distilled toluene, MeCN, and DMF in preparation for the steady-state and ultrafast measurements. The steady-state absorbance and fluorescence measurements were performed using 2 mm pathlength cuvette in a Cary 100 and a Cary Eclipse, respectively. The experimental apparatus used to collect femtosecond pump-probe transient spectra has been previously described<sup>23</sup>. Briefly, 100 fs, 1KHz, 800 nm pulses were generated by a Spectra-Physics Solstice Ti:Sapphire regenerative amplifier. The output of the Ti:Sapphire regenerative amplifier was used to pumping a Light Conversion TOPAS to produce spectrally tunable visible pulses and also to generate a white-light continuum probe using a sapphire plate. The output from the TOPAS was used for the tunable excitation or pump pulses and the white-light continuum was used for the probe. All measurements were made at room temperature.

## RESULTS AND DISCUSSION

Beginning with steady-state measurements, Figure 2 shows the absorption spectra of (a) TD1-Cu, and (b) TD1-Pd complexes as well as the oxidized (c) TD1-Cu-Ox and (d) TD1-Pd-Ox complexes dissolved in toluene, DMF, and MeCN. The absorption spectra of the neutral radical metal complexes in Fig. 2 (a) and (b) show two main bands in the visible at ~380 nm and ~600 nm. There are also two transitions with low oscillator strength in the near-IR at ~835 nm and ~900 nm (not shown), which are characteristic of ligand-based radicals of oligopyrrolic complexes. Ligand-only absorption spectra in the same solvents shows two main bands at ~320 nm and ~480 nm<sup>23</sup>. Previous work on linear oligopyrroles,<sup>8, 24</sup> a recent DFT calculation on a related linear tripyrrin,<sup>25</sup> as well as electrochemical measurements on the TD1-Pd complex<sup>16</sup> indicate that the two main bands originate from  $\pi$ - $\pi^*$  transitions. Both bands red-shift upon binding metal cations. This red-shift is consistent with ionochromic effects often observed in many metal-chelating

conjugated polymers containing pyridyl moieties.<sup>26-28</sup> The red-shift is thought to occur when metal ion coordination to a polymer leads to conjugation enhancement through rigidification and electron density variation in the polymer backbone. Metal ion coordination to three pyrrolic nitrogens in the tripyrrindione backbone is likely to cause similar effects as the lower energy band is narrower in the metal complex than in the free ligand, consistent with increased rigidity.

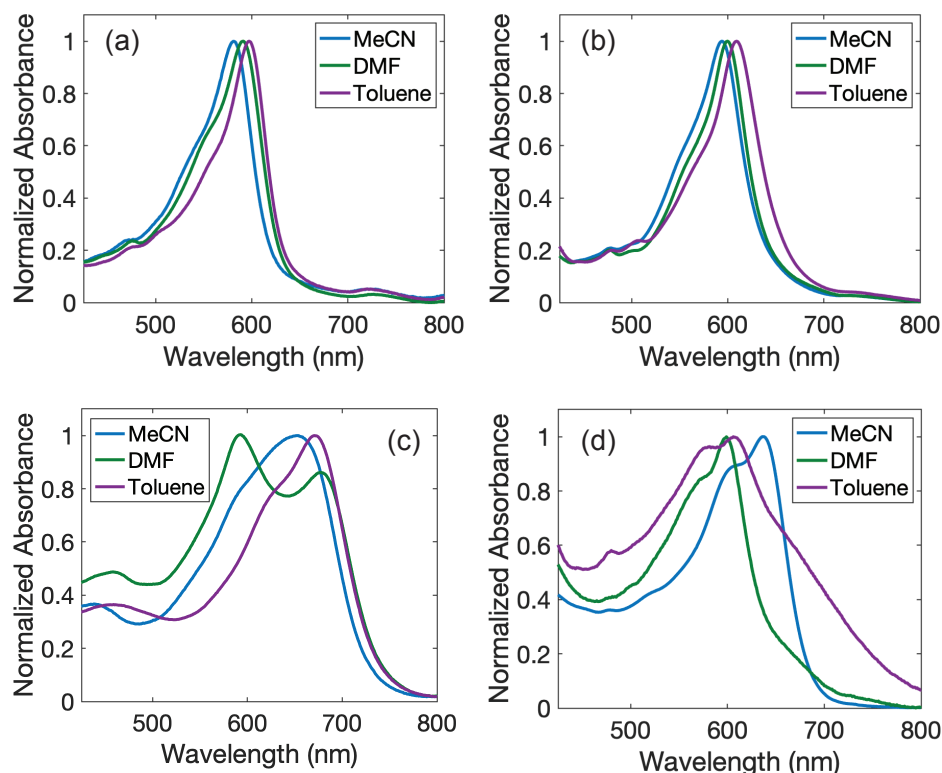


**Figure 2.** Normalized steady-state absorption spectra of neutral radical (a) TD1-Cu and (b) TD1-Pd complexes as well as the oxidized complexes (c) TD1-Cu-Ox and (d) TD1-Pd-Ox dissolved in toluene (purple), DMF (green), and MeCN (blue).

As shown in Figure 2 (a) and (b), the absorption spectra of the neutral radical complexes are only weakly solvent dependent. We did not observe polarity-dependent spectral shifts associated with charge-transfer states or changes in spectral features caused by axial coordination of solvent molecules. The largest shift observed for the transition at  $\sim 600$  nm was  $415\text{ cm}^{-1}$  for TD1-Pd, and

462  $\text{cm}^{-1}$  for TD1-Cu (in toluene and MeCN). In comparison, the free ligand has a larger solvatochromatic shift, where the difference between the peak maxima in the same two solvents is 854  $\text{cm}^{-1}$ , nearly double that of the TD1-Pd and TD1-Cu complexes.

The weak solvent effects displayed by the neutral radical metal ion complexes contrast with those observed for the oxidized form of the TD1-metal ion complexes, TD1-Cu-Ox and TD1-Pd-Ox, shown in Fig. 2 (c) and (d). The absorption spectra of the oxidized complexes have larger variations in band peak positions and broader lineshapes. The one-electron oxidation of both the copper and the palladium complexes removes an electron from the tripyrrindione creating a monoanionic tridentate ligand while maintaining the oxidation state of the metal<sup>16</sup>. Both the peak position and lineshape of the absorption spectra of the oxidized copper complexes are dependent on the solvent environment, although, neither the peak positions for TD1-Cu-Ox or TD1-Pd-Ox follow a general trend relative to the static dielectric constants of the solvents [toluene (2.38), MeCN (35.94), DMF (36.71)]. In DMF, the absorption spectrum of the oxidized complexes evolved as the samples aged in solution. This was likely due to the oxidized complex slowly reverting to the neutral radical form.

Steady-state excitation-emission scans for both metal complexes in all four solvents across the UV-Vis range showed no discernible photoluminescence. Fluorescence quenching in metal-bound porphyrins is well known when the metal centers are paramagnetic open-shell, such as  $\text{Cu}^{2+}$  ( $d^9$ ), or heavy metal diamagnetic closed-shell, such as  $\text{Pd}^{2+}$  ( $d^8$ ).<sup>29, 30</sup> DFT calculations of open- and closed-shell metal porphyrins identified a manifold of states below the  $\pi-\pi^*$  lowest energy excited state<sup>31</sup> which are thought to facilitate rapid relaxation.<sup>32-34</sup> In non-fluorescent Cu(II) porphyrin,<sup>35</sup> ligand-to-metal charge-transfer states greatly enable intersystem crossing into  $\pi-\pi^*$  triplet states and the subsequent recovery of the ground state.<sup>34-39</sup> The lack of fluorescence in Pd(II)



porphyrins is discussed in early experimental studies.<sup>29, 39-42</sup> It is likely that the metal ions similarly influence the fluorescence quenching in the TD1-metal complexes. Lowered symmetry DFT calculations on a closely related ligand, tripyrrin, show two bands, one Soret-like at ~350 nm and one Q-like at ~530 nm, for the  $\pi$ - $\pi^*$  states situating them at higher energies than typical Soret- and Q-band in porphyrins.<sup>25</sup> This makes metal-assisted deactivation likely since the metal d-orbital energies are likely similar when bound to TD1 or to porphyrin.<sup>43</sup>

Ultrafast relaxation dynamics were observed using broadband-probe transient absorption measurements. Representative data for the oxidized and neutral radical forms of the copper and palladium complexes is shown in Figure 3. The top row, panels (a), (b), and (c), presents the transient absorption spectra at selected time slices for copper complexes while the bottom row, panels (d), (e), and (f), presents the data for palladium complexes. Transient absorption data collected for additional solvent environments is presented in the ESI, Figures S1 and S2. The transient absorption measurements were performed exciting the lowest energy ligand  $\pi$ - $\pi^*$  transition that has significant oscillator strength. For the neutral radical complexes, laser pulses centered at 600 nm were used for excitation, while excitation pulses centered at 640 nm were used for TD1-Cu-Ox and TD1-Pd-Ox in MeCN, and 675 nm for TD1-Cu-Ox in toluene and TD1-Cu-Ox in DMF.

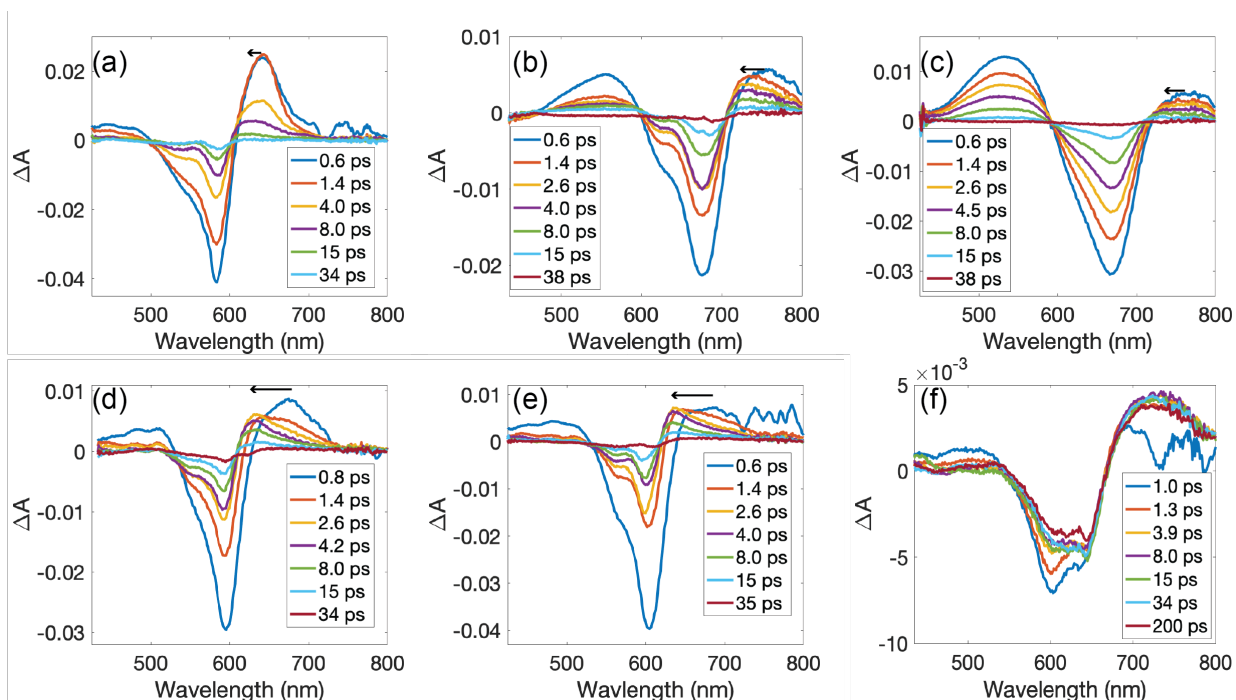


**Figure 3.** Transient absorption spectra of neutral radical and one-electron oxidized forms of the copper and palladium tripyrrindione complexes. The top row, panels (a), (b) and (c), presents data for copper complexes while the bottom row, panels (d), (e) and (f), presents data for palladium complexes. Panel (a) shows the transient absorption data for the neutral radical TD1-Cu complex in MeCN, (b) for the oxidized TD1-Cu-Ox complex in toluene, and (c) for the oxidized TD1-Cu-Ox complex in MeCN. Panel (d) shows the transient absorption data for the neutral radical TD1-Pd complex in MeCN, (e) for the neutral radical TD1-Pd complex in DMF, and (f) for the oxidized TD1-Pd-Ox complex in MeCN. The arrows indicate blue shifts. All data presented here was collected at room temperature.

All the TA data is characterized by a ground state bleach (GSB) at the energy of the main  $\pi-\pi^*$  transition as well as excited state absorption (ESA) contributions both at the high and low energy sides of the bleach. A feature associated with stimulated emission (SE) is not directly observed in the data although it may be hidden under the positive region to the low energy side of the ground

state bleach where there is a significant ESA contribution in all traces. The lack of SE contributions is consistent with the fact that we did not observe fluorescence for the complexes studied here.

As shown in Figure 3 (d) and (e), the transient absorption data obtained for the palladium neutral radical complex is relatively insensitive to solvent. The same insensitivity is observed for the copper neutral radical complex. The minimal effect of the solvent is also seen in the steady-state absorption data shown in Figure 2 (a) and (b). We observe the same solvent insensitivity in transient absorption data for both the palladium and copper oxidized complexes. Representative data for the oxidized copper complex is shown in Figure 3 (b) and (c) and for the oxidized Pd complex in panel (f). This is surprising given the spectral shifts observed for the oxidized complexes in the steady-state absorption (Figure 2 (c) and (d)). In addition to polarity and basicity, the solvents used here differ in viscosity, ranging from 0.347 mPa·s for MeCN to 0.94 mPa·s for DMF at 298 K. However, no significant effect due to varying viscosity, polarity or basicity was observed in the transient absorption data. These patterns indicate that the relaxation dynamics depend primarily on the identities of the metal centers and the overall oxidation state of the complex.

Representative transient absorption data for the copper neutral radical complex is shown in Figure 3 (a). It is characterized by a GSB around 585 nm (the negative-going peaks coincide with the peak of the main  $\pi-\pi^*$  transition), an ESA on either side of the bleach, one peaked  $\sim 645$  nm, and another having a flatter feature with smaller amplitude extending to the blue. The ESA features appear within our instrument response. The ESA and the GSB decay simultaneously in 10s of picoseconds. The transient absorption data was fit using global analysis<sup>22</sup> to identify common kinetic components. For TD1-Cu, two timescales were identified ranging from 1.7 to 2.4 ps, and from 7.8 to 13.2 ps. The timescales are listed in Table 1. Both ESA features rise within pulse

overlap. The higher energy ESA decays rapidly, followed by the near simultaneous decay of the GSB and the lower energy ESA. This occurs across all samples regardless of solvent. We observed a small amount of residual scatter from the pump excitation in all measurements. The ESA centered at 645 nm appears within the instrument response and undergoes a blueshift of approximately 15 nm, as indicated by an arrow in the figure. No blueshift is observed in the GSB.

Figure 3 (b) and (c) present transient absorption data for the oxidized copper complexes in toluene and MeCN respectively. The data is characterized by a GSB at the energy of the main  $\pi$ - $\pi^*$  transition as well as ESA contributions to both the high and low energy sides of the GSB feature. The ESA and the GSB decay simultaneously. A global analysis of the data across the three solvents here returned the following timescales: 1.5 to 2.3 ps and 10.7 to 11.5 ps. The timescales obtained from the global analysis are presented in Table 1. We observe a rapid blue shift in the ESA to the low energy side of the GSB centered at 740 nm of approximately 20 nm in all solvents that occurs in approximately 2 ps. No blueshift was observed in the GSB. Both ESA features and the GSB decay nearly simultaneously with little variation across solvents.

Transient absorption of the neutral radical TD1-Pd complex in MeCN and DMF is shown in Figure 3 (d) and (e), respectfully. From this data, two timescales were found in all three solvents, ranging 0.5–0.8 ps, and 7.4–11.4 ps. The timescales obtained from the global analysis are presented in Table 1. The initial spectrum following the instrument response shows a bleach around 600 nm and excited state absorption features on either side of the bleach, initially centered around at 475 nm and 690 nm. The 475 nm excited state absorption feature rapidly decays to zero while at the same time the 690 nm ESA undergoes a significant blue-shift of approximately 60 nm. No blue-shift was observed for the GSB. The remaining absorption and bleach features

simultaneously decay of within tens of ps to zero (the near zero non-decaying amplitude is associated with 600 nm pump scatter).

Figure 3(f) presents transient absorption data for the oxidized TD1-Pd-Ox complex in MeCN. Unlike the transient absorption data for the other molecules, the oxidized palladium complex has a long-lived excited state and undergoes little spectral evolution. The data shows a GSB centered at 620 nm, with two ESA contributions centered at 500 nm and 740 nm. Global analysis identified three timescales in the three solvents, 0.4–1.0 ps, 8–60 ps, and 3–6 ns, which are presented in Table 1. This last timescale is not well characterized by our experiment as it is longer than the maximum time delay. The ESA at 740 nm rises within the first 1.5 ps while the other ESA at 500 nm decays rapidly. The GSB decreases to about 1/3 of its initial value within tens of ps. The remaining GSB and the ESA centered at 740 nm do not decay out to 200 ps, which is the maximum measured delay time. No clear blue-shifts are identified in this data.

	<b>Toluene</b>	<b>DMF</b>	<b>MeCN</b>
<b>TD1-Cu</b>	2.3±0.3ps, 13.2±1.1ps	2.4±0.4ps, 7.8±1.2ps	1.7±0.2ps, 8.0±1.0ps
<b>TD1-Cu-Ox</b>	1.5±0.1ps, 10.7±0.8ps	2.0±0.2ps, 11.0±0.5ps	2.3±0.2ps, 11.5±0.6ps
<b>TD1-Pd</b>	0.8±0.1ps, 9.6±1.1ps	0.5±0.1ps, 7.4±1.0ps	0.6±0.1ps, 11.4±1.8ps
<b>TD1-Pd-Ox</b>	1.0±0.1ps, 60±3.1ps, 5*ns	0.4±0.1ps, 8±1.0ps, 6*ns	0.4±0.1ps, 40±2.0ps, 3*ns

Table 1. Lifetimes recovered from the global analysis performed on time-evolving transient spectra of TD1-Cu, TD1-Cu-Ox, TD1-Pd, and TD1-Pd-Ox reported with error bars generated from the standard error. \*ns timescale outside of maximum time delay of experiment.

For the copper complexes, the timescales obtained for the neutral radical and the oxidized species are similar in all solvents. The timescales for the neutral radical palladium complex are

faster but comparable to those found for the neutral radical copper molecules. The oxidized form of the palladium complex is an outlier. In all other molecules studied here, the transient absorption signal disappears, and the molecule returns to the ground state in tens of picoseconds. For TD1-Pd-Ox, there is a fast decay of the higher energy ESA and some relaxation of the bleach in tens of picoseconds, however, the excited state lifetime is significantly longer than the maximum time delay of the measurement (200 ps).

For the transient absorption data, the samples were excited in resonance with the lowest energy transition with significant oscillator strength, which is mainly localized on the ligand. The overall ligand dominance of the state is supported by experimental and computational observations. Comparison of the electrochemistry of the metal complexes indicates that the redox processes are occurring on the electron-rich conjugated  $\pi$  system of the ligand, with metal centers remaining in the same oxidation states.<sup>15, 16</sup> Metal coordination red-shifts and changes the spectral shape but the lack of solvent polarity dependence indicates a weak ligand–metal charge-transfer character. Previously published results<sup>15, 16</sup> indicate that while the metal center does have some involvement, the transitions primarily originate from the  $\pi$  system. EPR data further shows that the unpaired electron in the metal-bound neutral radical is delocalized over and accommodated by the ligand  $\pi$  system.<sup>16</sup>

The  $\pi$  to  $\pi^*$  nature of the primary transition in the visible means that redox or photophysical processes are relatively decoupled from the metal center. This potentially expands the types of processes that can be accommodated in a TD1-metal system, with those directly involving the metal center separated from the ligand. Although we do not observe it in our data, this could also involve chemical access to the metal center through the aqua ligand. In metalloporphyrins, the metal may participate in the dynamics by dissociating an axial ligand. For the TD1 complexes, the

coordinated aqua ligand is also hydrogen-bound to the tripyrrindione ligand and its unfavorable dissociation would be readily apparent from changes in the absorption spectra following the measurement. Since we do not observe these spectral changes and the complex is stable during the experiment, we can conclude that the water ligand is retained.

The similarities between the transient absorption data for TD1-Cu, TD1-Cu-Ox, and TD1-Pd as well as the different dynamics observed for TD1-Pd-Ox can be explored by considering the electronic states. As has been shown in previous work, in all the complexes studied here, the metal center is in a square planar geometry<sup>16, 17</sup>. In addition, the one-electron-oxidation of the complexes removes the electron from the ligand and not the metal center<sup>15</sup>. This means that the palladium complexes have a diamagnetic  $d^8$  Pd(II) center while the copper complexes have a paramagnetic  $d^9$  open-shell Cu(II) center with an unpaired electron. Both neutral radical complexes have an electron occupying the conjugated  $\pi$  orbitals on the ligand. For TD1-Pd, this means that the ground state is a doublet with a singly occupied molecular orbital (SOMO) primarily localized on the ligand. For the copper neutral radical complex, TD1-Cu, the picture is a bit more complicated. The unpaired electron on the  $d^9$  Cu(II) center is in the  $d_{x^2-y^2}$  orbital and is nearly orthogonal to the electron localized on the ligand<sup>15</sup>. The ferromagnetic interaction between these unpaired electrons results in a triplet ground state. This situation is not unique to TD1-Cu and has been observed for other Cu(II) metal centers coordinated with planar radical ligands<sup>44-50</sup>.

In the one-electron-oxidized complexes, the electron on the ligand is removed and the oxidation state of the metal center remains the same. For TD1-Cu-Ox, the unpaired electron on the copper results in a doublet ground state. The oxidized palladium complex, TD1-Pd-Ox, is a closed shell system with a square planar  $d^8$  Pd(II) metal center and the unpaired electron removed from the ligand. Of all the complexes studied here, TD1-Pd-Ox is the only one with a singlet state

and for which we observe a long excited-state lifetime. The tunability enabled by a delocalized electron on the ligand and the ability of TD1 to bind multiple metals provides a method to select the overall spin state of the complex and to adjust the dynamics of the system.

For each complex, the overall spin is expected to be conserved from the ground to the excited state. This is supported by the fast relaxation dynamics for TD1-Pd, TD1-Cu and TD1-Cu-Ox as well as the slower dynamics for the only species with a singlet ground state, TD1-Pd-Ox. For the neutral radical, TD1-Pd, it is possible that as a heavy metal, palladium could promote intersystem crossing. However, in Pd(II) porphyrin, the lifetime of the singlet state is on the order of tens of ps<sup>32</sup> and the triplet state has a minimum lifetime of hundreds of ps.<sup>51</sup> These are significantly longer timescales than those observed for TD1-Pd. Pd(II) porphyrins also generally have small Stokes shifts, on the order of 100-200 cm<sup>-1</sup>, which is significantly smaller than the shift observed here (approximately 1500 cm<sup>-1</sup>).

The fast relaxation observed for the copper complexes is most likely allowed by spin conserving transitions, with a triplet excited state for TD1-Cu and a doublet excited state for TD1-Cu-Ox. However, assuming that the orthogonality between the  $d_{x^2-y^2}$  orbital and the  $\pi$  orbital on the ligand is not complete, it is also possible that the unpaired electron on the d<sup>9</sup> Cu(II) metal center interacts with the  $\pi$  system altering  $\pi$  singlet and triplet multiplicity through an exchange interaction<sup>33, 34, 37, 52, 53</sup>. This would lead to fast intersystem crossing that could allow an excited state of different multiplicity.

As shown in Fig. 3 (and in Fig. S1 and S2 in the ESI), the transient absorption spectra for both neutral radical complexes and the oxidized copper complex undergoes spectral evolution. For these complexes, the lower energy ESA features shift to higher energy. The TD1-Pd signals have a significant 60 nm blue-shift of the 690 nm ESA feature. Both TD1-Cu and TD1-Cu-Ox have



relatively small, 15 nm and 20 nm, blue shifts of the ESA centered at approximately 645 nm and 740 nm, respectively. No blue shifts are observed for TD1-Pd-Ox. The spectral shift of an ESA to higher energies is generally associated with vibrational relaxation on the excited state<sup>54-58</sup>. Diffusive solvation processes or vibrational cooling driving the blue shift of the ESA features is also suggested by the narrowing of the ESA feature, which is observed for all data except TD1-Pd-Ox. This narrowing is most apparent in the TD1-Pd data (Fig. 3 (d), (e)). The picosecond timescales associated with the spectral blue-shift of the ESA are reasonable for solvation processes and vibrational cooling.

## CONCLUSION

Steady-state and femtosecond ultrafast time-resolved measurements were performed on copper and palladium complexes of tripyrrindione in both neutral radical and one-electron-oxidized forms. The steady-state and time-resolved spectra were found to be relatively insensitive to the solvent environment. Recovery of the ground state was observed within 10-100 ps for the copper and palladium neutral radical complexes as well as the oxidized copper complex, while the excited state lifetime of the oxidized palladium complex was significantly longer. Blue shifts of ESA contributions were observed, consistent with vibrational cooling on the excited state. Selection of the metal center and oxidation state of the complex allows for tuning of the overall spin of the ground and excited states. The stable open shell configurations and the reversible redox activity of these novel tripyrrolic systems has potential applications for exploring applications involving both magnetism and conductivity properties.

## SUPPORTING INFORMATION

Transient absorption measurements on the copper and palladium complexes in additional solvent environments (Figure S1 and S2).

## ACKNOWLEDGMENTS

The authors gratefully acknowledge financial support from the UAREN program and the National Science Foundation (CAREER grant 1454047 to ET). VH thanks Prof. Scott Saavedra and Prof. Marek Romanowski for providing facility time and support. Thanks to Clayton Curtis for helpful discussions. Funding for the facility was provided in part by NSF Major Research Instrumentation Grant 0958790.

## REFERENCES

1. Milgrom, L., *The Colours of Life: An Introduction to the Chemistry of Porphyrins and Related Compounds*. Oxford University Press: Oxford, 1997.
2. Mizutani, T.; Yagi, S., Linear Tetrapyrroles as Functional Pigments in Chemistry and Biology. *J. Porphyrins Phthalocyanines* **2004**, *8*, 226-237.
3. Doust, A. B.; Wilk, K. E.; Curmi, P. M.; Scholes, G. D., The Photophysics of Cryptophyte Light-Harvesting. *J. Photochem. Photobiol., A* **2006**, *184*, 1-17.
4. Krause, G. H.; Weis, E., Chlorophyll Fluorescence and Photosynthesis: The Basics. *Annu. Rev. Plant Physiol. Plant Mol. Biol.* **1991**, *42*, 313-349.
5. Cogdell, R. J.; Howard, T. D.; Isaacs, N. W.; McLuskey, K.; Gardiner, A. T., Structural Factors Which Control the Position of the Qy Absorption Band of Bacteriochlorophyll a in Purple Bacterial Antenna Complexes *Photosynthesis Research* **2002**, *74*, 135-141.
6. Hu, D. X.; Withall, D. M.; Challis, G. L.; Thomson, R. J., Structure, Chemical Synthesis, and Biosynthesis of Prodiginine Natural Products. *Chemical Reviews* **2016**, *116*, 7818-7853.
7. Perez-Tomas, R.; Vinas, M., New Insights on the Antitumoral Properties of Prodiginines. *Current Medicinal Chemistry* **2010**, *17*, 2222-2231.
8. Falk, H., *The Chemistry of Linear Oligopyrroles and Bile Pigments*. 1 ed.; Springer-Verlag Wien: 1989; Vol. 1.

9. Beruter, J.; Colombo, J.-P.; Schlunegger, U. P., Isolation and Identification of the Urinary Pigment Uroerythrin. *Eur. J. Biochem.* **1975**, *56* (1), 239-244.
10. Bröring, M., Beyond Dipyrins: Coordination Interactions and Templated Macrocyclizations of Open-Chain Oligopyrroles. In *Handbook of Porphyrin Science with Applications to Chemistry, Physics, Materials Science, Engineering, Biology and Medicine*, Vol 8: *Open-Chain Oligopyrrole Systems*, Kadish, K. M.; Smith, K. M.; Guillard, R., Eds. World Scientific: Singapore, 2010; Vol. 8, pp 343-501.
11. Tomat, E., Coordination Chemistry of Linear Tripyrroles: Promises and Perils. *Comments Inorg. Chem.* **2016**, *36* (6), 327-342.
12. Dey, S. K.; Datta, S.; Lightner, D. A., Tripyrrindiones and a Red-Emitting Fluorescent Derivative. *Monatsh. Chem.* **2009**, *140* (10), 1171-1181.
13. Roth, S. D.; Shkindel, T.; Lightner, D. A., Intermolecularly Hydrogen-Bonded Dimeric Helices. Tripyrrindiones. *Tetrahedron* **2007**, *63* (45), 11030-11039.
14. Tomat, E.; Curtis, C. J., Biopyrrin Pigments: From Heme Metabolites to Redox-Active Ligands and Luminescent Radicals. *Accounts of Chemical Research* **2021**, *54* (24), 4584-4594.
15. Gautam, R.; Astashkin, A. V.; Chang, T. M.; Shearer, J.; Tomat, E., Interactions of Metal-Based and Ligand-Based Electronic Spins in Neutral Tripyrrindione  $\pi$  Dimers. *Inorg. Chem.* **2017**, *56* (11), 6755-6762.
16. Gautam, R.; Loughrey, J. J.; Astashkin, A. V.; Shearer, J.; Tomat, E., Tripyrrindione as a Redox-Active Ligand: Palladium(II) Coordination in Three Redox States. *Angew. Chem., Int. Ed.* **2015**, *54* (49), 14894-14897.
17. Bahn Müller, S.; Plotzitzka, J.; Baabe, D.; Cordes, B.; Menzel, D.; Schartz, K.; Schweyen, P.; Wicht, R.; Bröring, M., Hexaethyltripyrrindione (H<sub>3</sub>Et<sub>6</sub>tpd): A Non-Innocent Ligand Forming Stable Radical Complexes with Divalent Transition-Metal Ions. *Eur. J. Inorg. Chem.* **2016**, *2016*, 4761-4768.
18. Bröring, M.; Prikhodovski, S.; Tejero, E. C., Free-Base Tripyrrins. *Chemical Communications* **2007**, *13* (8), 876-877.
19. Bröring, M.; Brandt, C. D., Tripyrrin - the Missing Link in the Series of Oligopyrrolic Ligands. *Chemical Communications* **2001**, *5*, 499-500.
20. Bröring, M.; Prikhodovski, S., Coordination Polymers from Metal Tripyrrins. *Zeitschrift Fur Anorganische Und Allgemeine Chemie* **2008**, *634* (14), 2451-2458.
21. Bröring, M., Coordination Polymers Built from Metal Tripyrrin Units. *Journal of Porphyrins and Phthalocyanines* **2008**, *12* (12), 1242-1249.
22. van Wilderen, L. J. G. W.; Lincoln, C. N.; van Thor, J. J., Modelling Multi-Pulse Population Dynamics from Ultrafast Spectroscopy. *Plos One* **2011**, *6* (3).
23. Swain, A.; Cho, B.; Gautam, R.; Curtis, C. J.; Tomat, E.; Huxter, V., Ultrafast Dynamics of Tripyrrindiones in Solution Mediated by Hydrogen-Bonding Interactions. *The Journal of Physical Chemistry B* **2019**, *123* (26), 5524-5535.
24. Bröring, M.; Prikhodovski, S.; Brandt, C. D.; Tejero, E. C.; Kohler, S., Monomeric and Polymeric Copper and Zinc Tripyrrins. *Dalton Trans.* **2007**, *2*, 200-208.
25. Wang, X.; Bai, F. Q.; Xie, M.; Hao, L.; Zhang, H. X., A Theoretical Investigation on the  $\pi$ -Conjugation Effect on the Structures and Spectral Properties of Tetrapyrrole Zinc Complexes. *Synth. Met.* **2015**, *210*, 258-267.
26. Liu, B.; Yu, W. L.; Pei, J.; Liu, S. Y.; Lai, Y. H.; Huang, W., Design and Synthesis of Bipyridyl-Containing Conjugated Polymers: Effects of Polymer Rigidity on Metal Ion Sensing. *Macromolecules* **2001**, *34* (23), 7932-7940.

27. Zhang, M.; Lu, P.; Ma, Y. G.; Shen, J. C., Metal Ionochromic Effects of Conjugated Polymers: Effects of the Rigidity of Molecular Recognition Sites on Metal Ion Sensing. *Journal of Physical Chemistry B* **2003**, *107* (27), 6535-6538.
28. Yasuda, T.; Yamaguchi, I.; Yamamoto, T., A New Soluble 1,10-Phenanthroline Containing pi-Conjugated Polymer: Synthesis and Effect of Metal Complexation on Optical Properties. *Adv. Mater.* **2003**, *15* (4), 293-296.
29. Gouterman, M., Spectra of Porphyrins. *Journal of Molecular Spectroscopy* **1961**, *6* (1), 138.
30. Gouterman, M., Optical Spectra and Electronic Structure of Porphyrins and Related Rings. In *The Porphyrins*, Dolphin, D., Ed. Academic Press: New York, 1978; pp 1-165.
31. Rosa, A.; Ricciardi, G., Quantum Chemical Studies on the Excited-State Deactivation Mechanism in Transition-Metal Tetrapyrroles. In *Handbook of Porphyrin Science with Applications to Chemistry, Physics, Materials Science, Engineering, Biology and Medicine*, Vol 22: *Biophysical and Physicochemical Studies of Tetrapyrroles*, Kadish, K. M.; Smith, K. M.; Guillard, R., Eds. 2012; Vol. 22, pp 169-234.
32. Kobayashi, T.; Straub, K. D.; Rentzepis, P. M., Energy Relaxation Mechanism in Ni(II), Pd(II), Pt(II) and Zn(II) Porphyrins. *Photochem. Photobiol.* **1979**, *29* (5), 925-931.
33. Straub, K. D.; Rentzepis, P. M.; Huppert, D., Picosecond Spectroscopy of Some Metalloporphyrins. *Journal of Photochemistry* **1981**, *17* (3-4), 419-425.
34. Kim, D.; Holten, D.; Gouterman, M., Evidence from Picosecond Transient Absorption and Kinetic-Studies of Charge-Transfer States in Copper(II) Porphyrins. *J. Am. Chem. Soc.* **1984**, *106* (10), 2793-2798.
35. Harriman, A., Luminescence of Porphyrins and Metalloporphyrins .3. Heavy-Atom Effects. *Faraday Transactions* **1981**, *77*, 1281-1291.
36. Rajapakse, G. V. N.; Soldatova, A. V.; Rodgers, M. A. J., Photophysical Behavior of Open-Shell, First-Row Transition Metal meso-Tetraphenyltetrabenzoporphyrins Insights from Experimental and Theoretical Studies. *Journal of Physical Chemistry B* **2010**, *114* (45), 14205-14213.
37. Ake, R. L.; Gouterman, M., Porphyrins 14. Theory for Luminescent State in Vo, Co, Cu Complexes. *Theoretica Chimica Acta* **1969**, *15* (1), 20-42.
38. Antipas, A.; Dolphin, D.; Gouterman, M.; Johnson, E. C., Porphyrins .38. Redox Potentials, Charge-Transfer Transitions, and Emission of Copper, Silver, and Gold Complexes. *J. Am. Chem. Soc.* **1978**, *100* (24), 7705-7709.
39. Magde, D.; Windsor, M. W.; Holten, D.; Gouterman, M., Picosecond Flash Photolysis: Transient Absorption in Sn(IV), Pd(II), and Cu(II) Porphyrins. *Chemical Physics Letters* **1974**, *29* (2), 183-188.
40. Allison, J. B.; Becker, R. S., Effect of Metal Atom Perturbations on the Luminescent Spectra of Porphyrins. *Journal of Chemical Physics* **1960**, *32* (5), 1410-1417.
41. Allison, J. B.; Becker, R. S., Metalloporphyrins - Electronic Spectra and Nature of Perturbations .3. Absorption Spectra and Solute-Solvent Interactions. *Journal of Physical Chemistry* **1963**, *67* (12), 2675-&.
42. Harriman, A., Luminescence of Porphyrins and Metalloporphyrins .2. Copper(II), Chromium(III), Manganese(III), Iron(II) and Iron(III) Porphyrins. *Journal of the Chemical Society-Faraday Transactions I* **1981**, *77*, 369-377.

43. Edington, M. D.; Diffey, W. M.; Doria, W. J.; Riter, R. E.; Beck, W. F., Radiationless Decay from the Ligand-to-Metal Charge-Transfer State in the Blue Copper Protein Plastocyanin. *Chemical Physics Letters* **1997**, 275 (1-2), 119-126.
44. Erler, B. S.; Scholz, W. F.; Lee, Y. J.; Scheidt, W. R.; Reed, C. A., Spin Coupling in Metalloporphyrin Pi-Cation Radicals. *J. Am. Chem. Soc.* **1987**, 109 (9), 2644-2652.
45. Chaudhuri, P.; Verani, C. N.; Bill, E.; Bothe, E.; Weyhermüller, T.; Wieghardt, K., Electronic Structure of Bis(o-iminobenzosemiquinonato)metal Complexes (Cu, Ni, Pd). The Art of Establishing Physical Oxidation States in Transition-Metal Complexes Containing Radical Ligands. *J. Am. Chem. Soc.* **2001**, 123 (10), 2213-2223.
46. Kahn, O.; Prins, R.; Reedijk, J.; Thompson, J. S., Orbital Symmetries and Magnetic Interaction Between Copper(II) Ions and the o-Semiquinone Radical. Magnetic Studies of (di-2-pyridylamine)(3,5-di-tert-butyl-o-semiquinonato)copper(II) perchlorate and bis(bis(3,5-di-tert-butyl-o-semiquinonato)copper(II)). *Inorganic Chemistry* **1987**, 26 (21), 3557-3561.
47. Benelli, C.; Dei, A.; Gatteschi, D.; Pardi, L., Electronic Structure and Reactivity of Dioxolene Adducts of Nickel(II) and Copper(II) Triazamacrocyclic Complexes. *Inorganic Chemistry* **1990**, 29 (18), 3409-3415.
48. Okazawa, A.; Hashizume, D.; Ishida, T., Ferro- and Antiferromagnetic Coupling Switch Accompanied by Twist Deformation around the Copper(II) and Nitroxide Coordination Bond. *J. Am. Chem. Soc.* **2010**, 132 (33), 11516-11524.
49. Ghorai, S.; Sarmah, A.; Roy, R. K.; Tiwari, A.; Mukherjee, C., Effect of Geometrical Distortion on the Electronic Structure: Synthesis and Characterization of Monoradical-Coordinated Mononuclear Cu(II) Complexes. *Inorganic Chemistry* **2016**, 55 (4), 1370-1380.
50. Konishi, S.; Hoshino, M.; Imamura, M., Triplet ESR Spectrum of the Copper Porphyrin Cation Radical. *J. Am. Chem. Soc.* **1982**, 104 (7), 2057-2059.
51. Eastwood, D.; Gouterman, M., Porphyrins: XVIII. Luminescence of (Co), (Ni), Pd, Pt complexes. *Journal of Molecular Spectroscopy* **1970**, 35 (3), 359-375.
52. Ha-Thi, M. H.; Shafizadeh, N.; Poisson, L.; Soep, B., An Efficient Indirect Mechanism for the Ultrafast Intersystem Crossing in Copper Porphyrins. *J. Phys. Chem. A* **2013**, 117 (34), 8111-8118.
53. Asano, M.; Kaizu, Y.; Kobayashi, H., The Lowest Excited-States of Copper Porphyrins. *Journal of Chemical Physics* **1988**, 89 (11), 6567-6576.
54. Bishop, M. M.; Roscioli, J. D.; Ghosh, S.; Mueller, J. J.; Shepherd, N. C.; Beck, W. F., Vibrationally Coherent Preparation of the Transition State for Photoisomerization of the Cyanine Dye Cy5 in Water. *The Journal of Physical Chemistry B* **2015**, 119 (23), 6905-6915.
55. Shaw, G. B.; Grant, C. D.; Shirota, H.; Castner, E. W.; Meyer, G. J.; Chen, L. X., Ultrafast Structural Rearrangements in the MLCT Excited State for Copper(I) bis-Phenanthrolines in Solution. *J. Am. Chem. Soc.* **2007**, 129 (7), 2147-2160.
56. Bilsel, O.; Milam, S. N.; Girolami, G. S.; Suslick, K. S.; Holten, D., Ultrafast Electronic Deactivation and Vibrational Dynamics of Photoexcited Uranium (IV) Porphyrin Sandwich Complexes. *The Journal of Physical Chemistry* **1993**, 97 (28), 7216-7221.
57. Jeong, D.; Kang, D.-G.; Joo, T.; Kim, S. K., Femtosecond-Resolved Excited State Relaxation Dynamics of Copper (II) Tetraphenylporphyrin (CuTPP) After Soret Band Excitation. *Scientific Reports* **2017**, 7 (1), 16865.
58. Marcelli, A.; Foggi, P.; Moroni, L.; Gellini, C.; Salvi, P. R., Excited-State Absorption and Ultrafast Relaxation Dynamics of Porphyrin, Diprotonated Porphyrin, and Tetraoxaporphyrin Dication. *The Journal of Physical Chemistry A* **2008**, 112 (9), 1864-1872.